



HAL
open science

The maize low-lignin *brown midrib3* mutant shows pleiotropic effects on photosynthetic and cell wall metabolisms in response to chilling

Catalina Duran Garzon, Michelle Lequart, Quentin Charras, Françoise Fournet, Léo Bellenger, Hélène Sellier-Richard, Catherine Giauffret, Wilfred Vermerris, Jean-Marc Domon, Catherine Rayon

► To cite this version:

Catalina Duran Garzon, Michelle Lequart, Quentin Charras, Françoise Fournet, Léo Bellenger, et al.. The maize low-lignin *brown midrib3* mutant shows pleiotropic effects on photosynthetic and cell wall metabolisms in response to chilling. *Plant Physiology and Biochemistry*, 2022, 184, pp.75-86. 10.1016/j.plaphy.2022.05.006 . hal-03686646

HAL Id: hal-03686646

<https://u-picardie.hal.science/hal-03686646>

Submitted on 22 Jul 2024

HAL is a multi-disciplinary open access archive for the deposit and dissemination of scientific research documents, whether they are published or not. The documents may come from teaching and research institutions in France or abroad, or from public or private research centers.

L'archive ouverte pluridisciplinaire **HAL**, est destinée au dépôt et à la diffusion de documents scientifiques de niveau recherche, publiés ou non, émanant des établissements d'enseignement et de recherche français ou étrangers, des laboratoires publics ou privés.



Distributed under a Creative Commons Attribution - NonCommercial 4.0 International License

The maize low-lignin *brown midrib3* mutant shows pleiotropic effects on photosynthetic and cell wall metabolisms in response to chilling

Catalina Duran Garzon¹, Michelle Lequart¹, Quentin Charasse², Françoise Fournet¹, Léo Bellenger^{1†}, Hélène Sellier-Richard³, Catherine Giauffret⁴, Wilfred Vermerris⁵, Jean-Marc Domon¹, Catherine Rayon^{#1}

¹UMR-INRAE 1158 Transfrontalière BioEcoAgro, BIOlogie des Plantes et Innovation (BIOPI), Université de Picardie Jules Verne, 80039, Amiens, France.

²UMR 7265 Aix Marseille Université, CEA, CNRS, BIAM, Laboratoire de génétique et biophysique des plantes, 13108 Saint Paul-Lez-Durance, France.

³ UMR-INRAE 1158 Transfrontalière BioEcoAgro, Unité Expérimentale Grandes Cultures Innovation et Environnement, Estrées-Mons, 80203 Péronne, France

⁴ UMR-INRAE 1158 Transfrontalière BioEcoAgro, AgrolImpact, Estrées-Mons, 80203 Péronne, France.

⁵Department of Microbiology & Cell Science; UF Genetics Institute; Florida Center for Renewable Chemicals and Fuels, University of Florida, Gainesville, FL 32610, USA.

† EA2106 Biomolécules et Biotechnologies Végétales, Faculté de Pharmacie, Université de Tours, Parc de Grandmont, 37200 Tours, France

#Corresponding author emails: catherine.rayon@u-picardie.fr

Abstract

Maize (*Zea mays* L.) is one of the major cereal crops in the world and is highly sensitive to low temperature. Here, changes in photosynthetic and cell wall metabolisms were investigated during a long chilling exposure in inbred line F2 and a low-lignin near-isogenic *brown midrib3* mutant (*F2bm3*), which has a mutation in the caffeic acid *O*-methyltransferase (*COMT*) gene. Results revealed that the plant biomass was reduced, and this was more pronounced in *F2bm3*. Photosynthesis was altered in both lines with distinct changes in photosynthetic pigment content between *F2bm3* and F2, indicating an alternative photoprotection mechanism between lines under chilling. Starch remobilization was observed in *F2bm3* while concentrations of sucrose, fructose and starch increased in F2, suggesting a reduced sugar partitioning in F2. The cell wall was altered upon chilling, resulting in changes in the composition of glucuronorabinoxylan and a reduced cellulose level in F2. Chilling shifted lignin subunit composition in *F2bm3* mutant to a higher proportion of *p*-hydroxyphenyl (H) units, whereas it resulted in lignin with a higher proportion of syringyl (S) residues in F2. On average, the total cell wall ferulic acid (FA) content increased in both genotypes, with an increase in ether-linked FA in *F2bm3*, suggesting a greater degree of cross-linking to lignin. The reinforcement of the cell wall with lignin enriched in H-units and a higher concentration in cell-wall-bound FA observed in *F2bm3* as a response to chilling, could be a strategy to protect the photosystems.

Keywords

bm3, caffeic acid *O*-methyltransferase, photosynthetic pigments, non-structural sugars, hydroxycinnamic acid, *Zea mays* L.

ABBREVIATIONS

bm3, *brown midrib3*; CAD, (hydroxy)cinnamyl alcohol dehydrogenase; CCR, cinnamoyl-CoA reductase; C4H2, cinnamate 4-hydroxylase²; 4CL2, 4-coumarate:CoA ligase²; *COMT*, caffeic acid *O*-methyltransferase; CCoAOMT, 4-caffeoyl-CoA *O*-methyltransferase; FA, ferulic acid; F5H, 5-hydroxyconiferyl aldehyde/alcohol 5-hydroxylase; G, guaiacyl; GAX, glucuronoarabinoxylan; H, *p*-hydroxyphenyl; HCA, hydroxycinnamates; MEP pathway, methylerythritol phosphate pathway; OPP, oxidative pentose-phosphate; PAD, pulsed amperometry detection; pCA, *p*-coumaric acid; S, syringyl.

1. Introduction

Maize (*Zea mays* L.) is a diploid annual C4 grass and the world's third most cultivated cereal crop used globally as a source of food, feed and fodder (Ranum et al., 2014). It can also be used for bioenergy production by hydrolyzing starch from the grain or cellulose from biomass into fermentable sugars that can be converted to biofuels as an alternative to fossil fuels (Torney et al., 2007; Vermerris et al., 2007, Torres et al., 2015). Biotic and abiotic stresses have major influences on plant development and biomass production in maize. Even though maize is originally a subtropical grass, maize has become an extensively cultivated crop in temperate regions like northern Europe and southern Canada (Ranum et al., 2014; Cholakova-Bimbalova and Vassilev, 2017). However, temperatures below 15°C, common in these regions early in the growing season, cause chilling stress that impacts growth of young maize plants (Leipner and Stamp 2008; Riva-Roveda et al., 2016). In young maize plants, chilling alters photosynthetic parameters such as a reduction in chlorophyll and photosystem efficiency. This is associated with changes in carbon metabolism such as an accumulation in non-structural sugars, including starch, sucrose and glucose (Riva-Roveda et al., 2016; Duran-Garzon et al., 2020). It has also been shown that the expression of genes involved in photoassimilate partitioning, including the gene encoding sucrose transporter SUT2, was reduced in the chilling-sensitive maize line S160 (*Z. mays* spp. *indentata*, dent) (Bilska-Kos et al., 2016). The plant cell wall plays a key role as a physical barrier against abiotic and biotic stress (Santiago et al., 2013; Le Gall et al., 2015). Nonetheless, low temperature can also affect cell wall properties

(Cabané et al., 2012; Le Gall et al., 2015). The plant cell is surrounded by a primary cell wall and in grass species, including maize, the primary cell wall consists of cellulose microfibrils embedded in a matrix of hemicelluloses (glucuronoarabinoxylan (GAX), xyloglucan, mixed linkage (1→3), (1→4)-β-D-glucan) and pectin (Carpita and Gibeaut, 1993; Carpita et al., 2001; Santiago et al., 2013). Once cell elongation has ceased, a secondary cell wall is formed, which can be lignified in some specific tissues (xylem, sclerenchyma) (Barros et al., 2015). GAX is a typical polysaccharide of commelinid monocotyledons that consists of a backbone of (1,4)-linked β-D-xylopyranosyl residues mostly substituted with a single α-L arabinose residue at O3, but in the endosperm it can also be di-substituted at O2 and O3 (Scheller and Ulvskov, 2010). The xylose residues can also be substituted by α-D-glucuronic acid and 4-O-methyl glucuronosyl residues at the O2 or O3 position (Peña et al., 2016). Hydroxycinnamic acids such as FA and *p*-coumaric (pCA) acids can be ester-linked to O5 of some arabinofuranosyl residues of GAX (de Oliveira et al., 2015). FA residues can be oxidatively cross-linked to each other to form dimers (Ralph et al., 1995) that can cross-link different GAX polymers. FA can also be ether-linked to lignin, enabling the crosslinking of GAX and lignin (Ralph et al., 1995; de O. Buanafina, 2009; de Oliveira et al., 2015). Lignin is a phenolic biopolymer consisting of *p*-hydroxyphenyl (H), guaiacyl (G) and syringyl (S) units that is formed in the secondary wall via oxidative coupling of three different monolignols, *p*-coumaryl, coniferyl and sinapyl alcohol, respectively (Boerjan et al., 2003; Ralph et al., 2004; Barros et al., 2015). In maize and other grasses these monolignols are synthesized from the amino acids L-phenylalanine and L-tyrosine by the enzymes of the phenylpropanoid pathway (Rösler et al., 1997; Barros et al., 2016; Jun

et al., 2018), followed by several monolignol-specific enzymes: cinnamoyl-CoA reductase (CCR), coniferyl aldehyde/alcohol 5-hydroxylase (known as ferulate 5-hydroxylase (F5H), 5-hydroxyconiferyl aldehyde/alcohol *O*-methyltransferase (known as caffeic acid *O*-methyltransferase (COMT), EC 2.1.1.6) and (hydroxy)cinnamyl alcohol dehydrogenase (CAD, E.C. 1.1.1.195), (Boerjan et al., 2003; Vanholme et al., 2010; Vermerris and Abril, 2015).

Maize is one the primary feedstuffs used for ruminant animals (Barrière, 2017). The cell wall contained in crop roughage can be lignified and lignification is a limitation of the cell wall digestion in the rumen (Méchin et al., 2005; Jung et al., 2012). The presence of lignin also contributes to the recalcitrance of biomass to the conversion to fermentable sugars (Zeng et al., 2012; Fu et al., 2011; McCann and Carpita, 2015). To improve the digestibility of maize biomass in ruminant animals or during biomass processing in biorefineries, *brown-midrib* mutants have provided greater roughage digestibility or improved saccharification (Barrière et al., 1994; Vermerris et al., 2007). Furthermore, transgenic technologies using antisense constructs mostly focused on two lignin biosynthetic pathway enzymes, CAD and COMT, to down regulate lignin biosynthesis have been undertaken as well (Piquemal et al., 2002; Guillaumie et al., 2008). COMT is involved in the formation of syringyl units *via* methylation of 5-hydroxyconifer aldehyde/5-hydroxyconiferyl alcohol. The maize *bm3* mutant, which contains a retrotransposon insertion in exon 2 of the *COMT* gene (*Zm00001d049541*) (Vignols et al., 1995) contains less lignin and less esterified pCA, and has a reduction in the S/G ratio (Chabbert et al., 1994; Marita et al., 2003), thus improving the cell wall digestibility (Barrière et al., 1994; Fontaine et al., 2003; Barrière et al., 2017).

Thus, alterations to cell wall metabolism could provide valuable tools for further improvement of maize biomass production. Due to climate change, it may be possible to plant maize earlier in the spring as a mechanism to avoid drought stress during summer. However, the economic losses of crops are greater if plants are subjected to stress at the juvenile stage. Therefore, chilling tolerance at the early stages of development is an important agronomic character.

In our study, we attempted to understand changes in photosynthesis and cell wall metabolisms in the *bm3* mutant in an F2 inbred background at a juvenile stage of development after a long chilling exposure. Our hypothesis was that the F2*bm3* mutant would be more chilling sensitive than the wild-type F2 line. Both F2 and F2*bm3* lines were grown under a long chilling treatment (60 days; 15°C days, 11°C nights) and compared to control conditions without chilling. The middle third of the fully elongated 4th leaf blade was harvested and the photosynthetic pigments, non-structural sugar content and cell wall composition were determined. Our data showed that reduced *COMT* gene expression induced specific changes in photosynthetic pigments and cell wall composition. However, these changes observed in F2*bm3* did not provide a better chilling tolerance than in the F2 line, indicating that a lower proportion of S-residues does not contribute to chilling tolerance in plants at a juvenile stage of development.

2. Material and methods

2.1. Plant material and growth conditions

The wild-type maize inbred line F2 and the near-isogenic *bm3* mutant (F2*bm3*) were provided by INRAE, IJPB (Méchin et al., 2000). The seeds were germinated in Petri

dishes between two wet blotting papers at 20 °C in darkness for 4 days before transplantation into pots filled with Klasmann TS3 (607) potting soil. Plants were grown as described in Duran-Garzon et al (2020). Plants were grown under controlled greenhouse conditions at INRA Estrées-Mons under two temperature scenarios: a standard temperature (25°C day / 22°C night for 21 days) and a low-temperature chilling treatment (15°C day / 11°C night for 60 days). The plants received supplementary light from Philips son-T 400-W sodium lamps (Philips Lighting UK, Surrey, UK) when the global solar radiation outside the greenhouse fell below 120 W m⁻². The plants were sampled at the V4 stage, i.e. when the 4th leaf had fully emerged. A total of 18 homogenous plants were harvested per genotype (F2 vs F2*bm3*), per biological replicate and growing condition (control vs. chilling). For each combination of condition, genotype and replicate, two representative plants were chosen for both photosynthesis and biomass measurements, while the 16 other plants were dedicated to leaf sampling. Leaf tissue was sampled 4 hours after the beginning of the light period, in the center segment of youngest fully-emerged expanded blade, outside the midrib. Samples from the 16 plants were bulked, frozen in liquid nitrogen, ground to a fine powder in a ball mill and kept frozen until further use (-80 °C). For each assay three biological replicates were analyzed, each consisting of pooled samples from 16 plants.

2.2. Biomass and plant growth

At each leaf sampling, the aerial biomass of two plants (without roots) per replicate, condition and genotype, was measured. Their fresh weight was determined immediately, while the dry weight was determined after oven drying at 80°C for 48h.

The plant height of 10 plants among the 18 selected plants was determined from digital images using ImageJ software (National Institutes of Health). Height was defined as the distance between the ligule of the 4th fully emerged leaf to the base of the plant. Both parameters were recorded for controlled and chilling conditions by three biological replicates.

2.3. Evaluation of chilling damage

To evaluate the effect of chilling on the aerial parts of the maize plants at the V4 stage a vigor score was assigned, which ranged from 0 (dead plants), 1-2 (high degree of chlorosis and surface lesion of the leaves), 3-4 (low degree of chlorosis and surface lesion of the leaves) to 5 (uninjured).

2.4. Measurement of photosynthetic parameters and pigment analyses

Photosynthetic parameters measurements were performed on the last fully expanded leaf of two plants per genotype, condition and replicate as described in Duran-Garzon et al. (2020).

For pigment content, 100 mg of ground frozen leaves was extracted in methanol according to Riva-Roveda et al. (2016) containing 0.01 mg/mL of canthaxanthine (Sigma-Aldrich) as internal standard for quantification. The pigments were separated by reverse phase high-performance liquid chromatography (Shimadzu), using a Zorbax Eclipse PAH column (4.6 × 150 mm, 3.5 μ pore size, Agilent) and a SPD-M20A diode array detector as described by Edelenbos et al. (2001). Commercial pigments (violaxanthin, antheraxanthin, zeaxanthin, chlorophyll *a* and *b* and β-carotene)

standards from DHI-Water and Environment (Horstholm, Denmark) were used for calibration.

2.5. Non-structural carbohydrates analyses and amylase activity measurement

Glucose, fructose, sucrose and starch content were extracted from ground frozen leaves (50 mg) according to De Souza et al. (2013). Samples were extracted 4 times in 1 mL of 80% (v/v) ethanol at 80°C for 20 minutes. The extract was centrifuged at 10 000 *g* for 5 minutes at room temperature and the supernatants were pooled, speed-vacuum dried and resuspended in 1 mL of water. The soluble fraction, which corresponds to the soluble sugars, was analyzed using high performance anion exchange chromatography with pulsed amperometric detection (HPAEC/PAD) (Dionex, CA, USA) on a Carbowac PA1 column as described by De Souza et al. (2013). Starch was quantified from the pellet obtained after ethanol extraction using Megazyme® (Bray, Co. Wicklow, Ireland) total starch assay procedure. Briefly, the pellet was washed with water and speed-vacuum dried for 1 h at 60°C. The pellet was then resuspended in 500 µL 2M KOH and incubated at 4°C for 20 min. A sodium acetate (100 mM, pH 5) buffer (200 µL) was added to the sample and twice digested with 50 µL of α-amylase (3000 U / mL) at 75°C for 30 min. The sample was further digested twice with 50 µL amyloglucosidase (3300 U / mL) and incubated at 50°C for 30 min. The reaction was stopped by adding 100 µL of 0.8 M perchloric acid and the supernatant was centrifuged at 10 000 *g* for 5 min at room temperature. The supernatant was used to determine the glucose concentration using a glucose assay (Megazyme®, Bray, Co. Wicklow, Ireland) according to the manufacturer's instructions.

Total amylase activity was determined according to the assay described by Cui et al. (2002) with minor modifications. Fine powder of maize (100 mg) was homogenized in 1.6 mL of 0.1 M phosphate buffer (pH 6.8). The homogenate was centrifuged at 12 000 *g* for 10 min. One milliliter of 0.1 M phosphate buffer (pH 6.8), 1 mL of 0.3% (w/v) NaCl, and 1 mL of 0.5% (w/v) starch (Megazyme total starch assay) buffers were successively added to 0.2 mL of supernatant in a test tube and mixed thoroughly. After incubation in a water bath for 5 min at 37°C, the reaction was stopped by adding 1 mL of 2.5 M NaOH buffer. The blank control was prepared as above, except that the starch solution was replaced with distilled water. The standard samples were set with six levels of glucose (0, 0.5, 1.0, 2.0, 3.0 and 4.0 mg/mL). The released reducing sugars were then determined according to the instructions of the manufacturer.

2.6. Cell wall sugar composition

Ground frozen leaves (150 mg) were homogenized in 1.6 mL ethanol and incubated at 70°C for 15 min. After centrifugation (10000 *g*, 5 min), the supernatant was discarded, and a second extraction was carried out. The pellet was further homogenized in 1.8 mL of 1%(w/v) SDS in 50 mM Tris-HCl, pH 7.2 buffer and incubated at 70°C for 30 min. After centrifugation (10000 *g*, 5 min), the supernatant was discarded, and the pellet was washed successively with H₂O, ethanol, acetone and H₂O again. The pellet was freeze dried and corresponded to the dry cell wall (DCW). DCW material was subjected to amylase treatment according to Fleischer et al. (1999) to remove starch. After digestion, 1 mg of destarched DCW was hydrolyzed by 4 N trifluoroacetic acid (TFA) at 100°C for 4 hours and TFA was evaporated under a stream of nitrogen. Samples were dissolved in 1 mL H₂O and 100 µL were injected onto a CarboPac-1 column (Dionex) HPAEC and

non-cellulosic sugars were separated and detected by pulsed amperometry (PAD). Neutral monosaccharides were separated using a mobile phase composed of solvent A = H₂O, solvent B = 160 mM NaOH and solvent C = 200 mM NaOH. The elution gradient was as follows: 0–25 min 90% A and 10% B, 25–26 min 0–100% C, 26–35 min 100% C, 25–36 min 100–0% C, 36–50 min 90% A and 10% B. For uronic acids quantification, the mobile phases were (A) 160 mM NaOH and (B) 600 mM NaOAc in 160 mM NaOH. The elution profiles were as follows: 0–5 min 100% A, 5–35 min 0–100% B, 35–40 min 100% B, 40–42 min 100–0% B and finally column re-equilibration by 100% A from 42 to 50 min. The flow rate was 1 mL/min and the column at 30°C. Data were collected and processed using the Chromeleon® 6.50 software (Dionex Corp.).

The concentration of (1→3),(1→4)-β-D-glucans from ground frozen leaves was quantified with a β-glucan detection kit from Megazyme® (Bray, Co. Wicklow, Ireland) as described in Domon et al. (2013). Analyses were performed in triplicate for each culture condition and each genotype.

Cellulose was quantified from the TFA pellet as an acetic-nitric acid-resistant material as described in Foster et al., (2010b). Cellulose content was determined in triplicate for each growth culture condition and each genotype.

2.7. Lignin assay and enzymatic assays

Lignin content was determined from 100 mg ground tissue of the 4th leaf using the acetyl bromide method initially described by Hatfield et al. (1999) with the modifications from Domon et al. (2013). Lignin subunit composition was determined on 2.5 mg DCW samples using thioacidolysis (Lapierre and Rolando, 1988) with the modifications from

Foster et al. (2010a). Samples were analyzed by injecting 1 μL on a Bruker 456 gas chromatograph (Bellerica, MA) equipped with a Restek Rxi-5ms column (30 m, 0.25 mm i.d., 0.25 μm film thickness; Restek Corp., Bellefonte, PA), which was connected to a Bruker Scion triple quadrupole mass spectrometer. The injector was set at 250°C and operated in splitless mode. The initial column temperature was 130°C, which was maintained for 3.0 min. The temperature was then increased to 270°C (15°C min⁻¹), with a final 2-min. hold. The transfer line was maintained at 250°C. Electron impact ionization was used with 70 eV electrons. The m/z range was set from 50-350, with a scan speed of 500 ms. Ions with m/z values of 239, 269 and 299 were diagnostic of thioacidolysis products derived from H-, G- and S-residues, respectively. Data were analyzed in Bruker Daltonics MS WorkStation software v. 8.2.1.

Enzymatic assays of CAD activity were determined from extracts obtained from ground frozen 4th leaves according to Domon et al. (2013).

2.8. Analysis of cell wall bound hydroxycinnamic acids

Hydroxycinnamic acids (*p*-coumaric and ferulic acid) linked to the cell walls by ester and ether bonds were determined by alkaline hydrolysis based on Sun et al. (2002) and Culhaoglu et al. (2011). Esterified hydroxycinnamic acids were released from dry cell wall samples (7 mg) by alkaline hydrolysis (2 mL of 2 M NaOH, 35°C, 2 h). Total esterified and etherified hydroxycinnamic acids were released using severe alkaline treatment (2 mL of 4 M NaOH, 170°C for 2 h in a dry bath). The hydrolysates were acidified to pH 2 with 4 M HCl and then extracted twice with 5 mL ethyl acetate (99.8%). The ethyl acetate extracts were then evaporated under nitrogen and dissolved in 1 mL

of methanol with 0.5 mg/mL ethyl vanillin as internal standard. The samples were analyzed using a Prominence Ultra-Fast Liquid Chromatograph (Shimadzu Prominence, Kyoto, Japan) equipped with a GraceSmart RP 18 (5 μ m, 250 mm \times 4.6 mm, GRACE). The column temperature was set at 25°C. The mobile phase consisted of H₂O (A) and CH₃CN (B), both in 0.1% formic acid. The injection volume was 5 μ L with a flow rate of 0.8 mL/min using a gradient program of 50 min as follows: initial A:B (95:5); 0–5 min linear change to A:B (91:9); 5–22 min linear change to A:B (9:11); 22–38 min linear change to A:B (11:18) and maintained for 2 min at 18%; 40–41 min linear change to A:B (18:80) and maintained for 4 min at 80%; 45–46 min linear change to A:B (95:5) and maintained for 4 min at 5%. Detection was carried out at 280 nm using an SPD-M20A photodiode array UV-VIS detector. Data were collected and processed using the Lab solutions (LC solutions) software. The concentration of ether-linked hydroxycinnamic acids was calculated as the difference between total and ester-linked hydroxycinnamic acids.

2.9. Statistical analysis

Statistical analyses were performed with R software (<http://www.R-project.org/>). Tukey's honest significant difference (HSD) statistic was used to compare means at $\alpha < 0.05$ between combinations of treatments and genotypes, as described in Duran-Garzon et al. (2020).

3. RESULTS

3.1. A long chilling treatment affects plant growth and development

To assess the role of *COMT* in maize growth and development under chilling treatment, plant height, chilling injury in the aerial parts of the plant, and biomass were estimated at the juvenile stage. Under controlled growth conditions, the *F2bm3* plants were slightly taller than the wild-type F2 plants, but both lines were significantly smaller under chilling treatment. Indeed, plant height was reduced by an average of 48% and 40% in *F2bm3* and F2 plants, respectively (**Fig. 1a**). That reduction in plant growth was correlated to aerial biomass. The dry aerial biomass was more reduced in *F2bm3* (57%) than in its wild-type counterpart F2 (32%) (**Fig. 1b**). The chilling injury in the aerial portions of the plants ranging from 0 (dead plants) to 5 (uninjured) was determined and showed that both *F2bm3* and F2 were chilling tolerant with a score of 4 (**Fig. S1**).

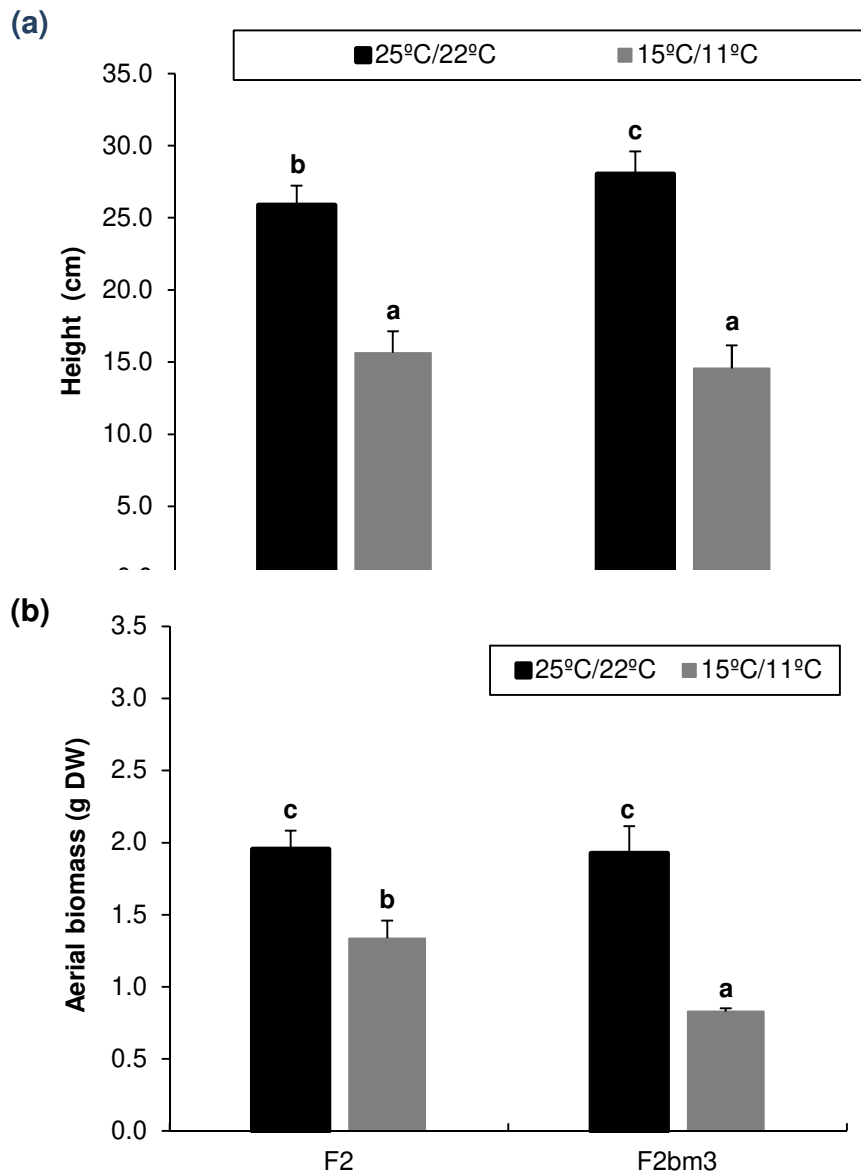


Figure 1. Chilling effects on plant growth and biomass in the low-lignin maize mutant *F2bm3* and the wild-type *F2* line. (a) Plant height of seedlings at the V4 stage under ambient growth conditions (black bar) and chilling stress (grey bar). (b) The average of aerial biomass (Dry Weight) after 45 days of chilling stress with a day/night temperature regime of 15°C/11°C. Data are means \pm SD (n=3). Means followed by a different letter in the same graph are statistically significantly different according to Tukey's test (P<0.05).

3.2. β -carotene is twice more abundant in F2bm3 than in F2 under chilling exposure.

Since chilling has a negative effect on photosynthesis in maize (Riva-Roveda et al., 2016), photosynthetic metabolism were assessed by measuring the photosynthetic pigments (**Table 1**).

Under normal growth conditions, F2 and F2bm3 displayed a similar amount of total chlorophyll. When plants were exposed to chilling, the chlorophyll a/b ratio increased by 33% in F2bm3 as a result of the lower abundance of chlorophyll b and photosynthesis efficiency (**Table 1**).

Table 1. Content of photosynthetic pigments at 25°C/22°C and 15°C/11°C in the 4th leaf of F2 and F2bm3 seedlings at the V4 stage. Data are means \pm SD (n=3). Means followed by different letters are significantly different according to Tukey's test (P<0.05). Chlorophyll (Chl).

Pigment	F2		F2bm3	
	25°C/22°C	15°C/11°C	25°C/22°C	15°C/11°C
	Mean \pm SD	Mean \pm SD	Mean \pm SD	Mean \pm SD
<i>Chl a</i> ($\mu\text{mol.g}^{-1}\text{FW}$)	1.20 \pm 0.2 a	1.43 \pm 0.4 a	1.49 \pm 0.1 a	1.43 \pm 0.1 a
<i>Chl b</i> ($\mu\text{mol.g}^{-1}\text{FW}$)	0.30 \pm 0.0 a	0.36 \pm 0.1 ab	0.49 \pm 0.0 b	0.35 \pm 0.0 ab
<i>Chl a+b</i> ($\mu\text{mol.g}^{-1}\text{FW}$)	1.50 \pm 0.2 a	1.79 \pm 0.4 a	1.98 \pm 0.1 a	1.78 \pm 0.2 a
<i>Chl a/b</i>	4.00 \pm 0.3 b	3.95 \pm 0.1 b	3.05 \pm 0.4 a	4.07 \pm 0.1 b
<i>Antheraxanthin</i> ($\mu\text{mol.g}^{-1}\text{FW}$)	0.01 \pm 0.0 a	0.07 \pm 0.0 c	0.01 \pm 0.0 a	0.03 \pm 0.0 b
<i>Zeaxanthin</i> ($\mu\text{mol.g}^{-1}\text{FW}$)	0.00 \pm 0.0 a	0.02 \pm 0.0 b	0.00 \pm 0.0 a	0.07 \pm 0.0 c
<i>Neoxanthin</i> ($\mu\text{mol.g}^{-1}\text{FW}$)	0.50 \pm 0.0 a	0.75 \pm 0.1 b	0.42 \pm 0.1 a	0.34 \pm 0.1 a
<i>Lutein</i> ($\mu\text{mol.g}^{-1}\text{FW}$)	0.37 \pm 0.0 c	0.36 \pm 0.0 c	0.28 \pm 0.0 b	0.19 \pm 0.0 a
<i>Violaxanthin</i> ($\mu\text{mol.g}^{-1}\text{FW}$)	0.33 \pm 0.0 bc	0.38 \pm 0.1 c	0.26 \pm 0.1 ab	0.22 \pm 0.0 a
<i>Xanthophyll</i> ($\mu\text{mol.g}^{-1}\text{FW}$)	1.21 \pm 0.0 b	1.58 \pm 0.2 c	0.97 \pm 0.1 ab	0.85 \pm 0.1 a

β -Carotene ($\mu\text{mol.g}^{-1}\text{FW}$)	0.76 \pm 0.0 <i>b</i>	0.35 \pm 0.1 <i>a</i>	0.84 \pm 0.1 <i>b</i>	0.75 \pm 0.0 <i>b</i>
Carotenoid ($\mu\text{mol.g}^{-1}\text{FW}$)	1.97 \pm 0.1 <i>b</i>	1.92 \pm 0.2 <i>ab</i>	1.81 \pm 0.1 <i>ab</i>	1.60 \pm 0.1 <i>a</i>

The carotenoid content was lower in *F2bm3* (~13%) and this trend remained unchanged under chilling exposure. This was related to xanthophyll pigments (antheraxanthin, zeaxanthin, neoxanthin), which increased by 30% in F2 in response to chilling. Specifically, in the F2 line, neoxanthin, which is a precursor of acid abscisic acid (ABA), a ubiquitous stress hormone, increased by 34%, while it remained unchanged in *F2bm3*. Lutein, another xanthophyll, was steady in F2, while it decreased by 33% in *F2bm3*. The β -carotene content was similar in both F2 and *F2bm3* plants under control conditions. It remained unchanged in the mutant under chilling exposure, while it was reduced by 50% in F2. The β -carotene/lutein ratio was 1.5-fold greater in *F2bm3* than in F2 under normal growth conditions. This ratio decreased by 50% in F2, while it increased by 30% in *F2bm3* under exposure to chilling. The higher chl *a/b* ratio and β -carotene content observed in *F2bm3* could be a metabolic response to chilling. In contrast to *F2bm3*, the high level of xanthophyll including lutein and neoxanthin observed in F2, could be a strategy to maintain a photoprotection under chilling exposure. Taken together, these data indicate that chilling changes the content of photosynthetic pigments in both genotypes, presumably to provide a better photoprotection, and that these changes are distinct for each line. Furthermore, the parameters of the functional state of the photosystems were determined (**Table S1**). Among the leaf photosynthetic parameters measured, the non-photochemical quenching (Φ_{NPQ}) and the constitutive thermal dissipation ($\Phi_{f,D}$) increased

significantly in both genotypes following exposure to chilling, indicating an alteration in photosynthesis.

3.3. The *F2bm3* mutant remobilizes starch under chilling exposure

Carbohydrate metabolism was characterized by determining the non-structural sugar content. *F2bm3* contained the highest amount of non-structural sugars, ($\sim 23 \text{ mg.g}^{-1}$ FW *F2bm3* vs $\sim 14 \text{ mg.g}^{-1}$ FW F2) under normal growth conditions (**Table S2**). Starch was by far the most abundant non-structural sugar in both lines and *F2bm3* contained more starch than F2 (22 mg.g^{-1} FW *F2bm3* vs 13 mg.g^{-1} FW F2) (**Fig. 2a**). When the plants were exposed to chilling, the starch content was reduced by 26% in *F2bm3* compared to an increase by 20% in F2. However, these changes resulted in a similar starch content in both lines. The starch content was well correlated with alpha-amylase enzyme activity (**Fig. S2**). The activity was 30% lower in *F2bm3* than in F2 under control conditions. The enzyme activity did not change in F2, while it increased by 27% in *F2bm3* under chilling which could explained the lower level of starch in *F2bm3*. The sucrose and fructose content was similar in both genotypes, but the glucose content was 1.7-fold greater in F2 compared to *F2bm3* under control conditions (**Fig. 2b**). The sucrose and fructose level remained similar in the *F2bm3* mutant, while it increased by 25% and 62% in F2, respectively, under chilling. The glucose concentration did not change significantly in response to chilling in either of the lines, although the average in *F2bm3* trended slightly higher was observed, which could arise from starch degradation.

The data indicate that F2 accumulates more soluble sugars, which may be used as osmoprotectants to maintain cell homeostasis.

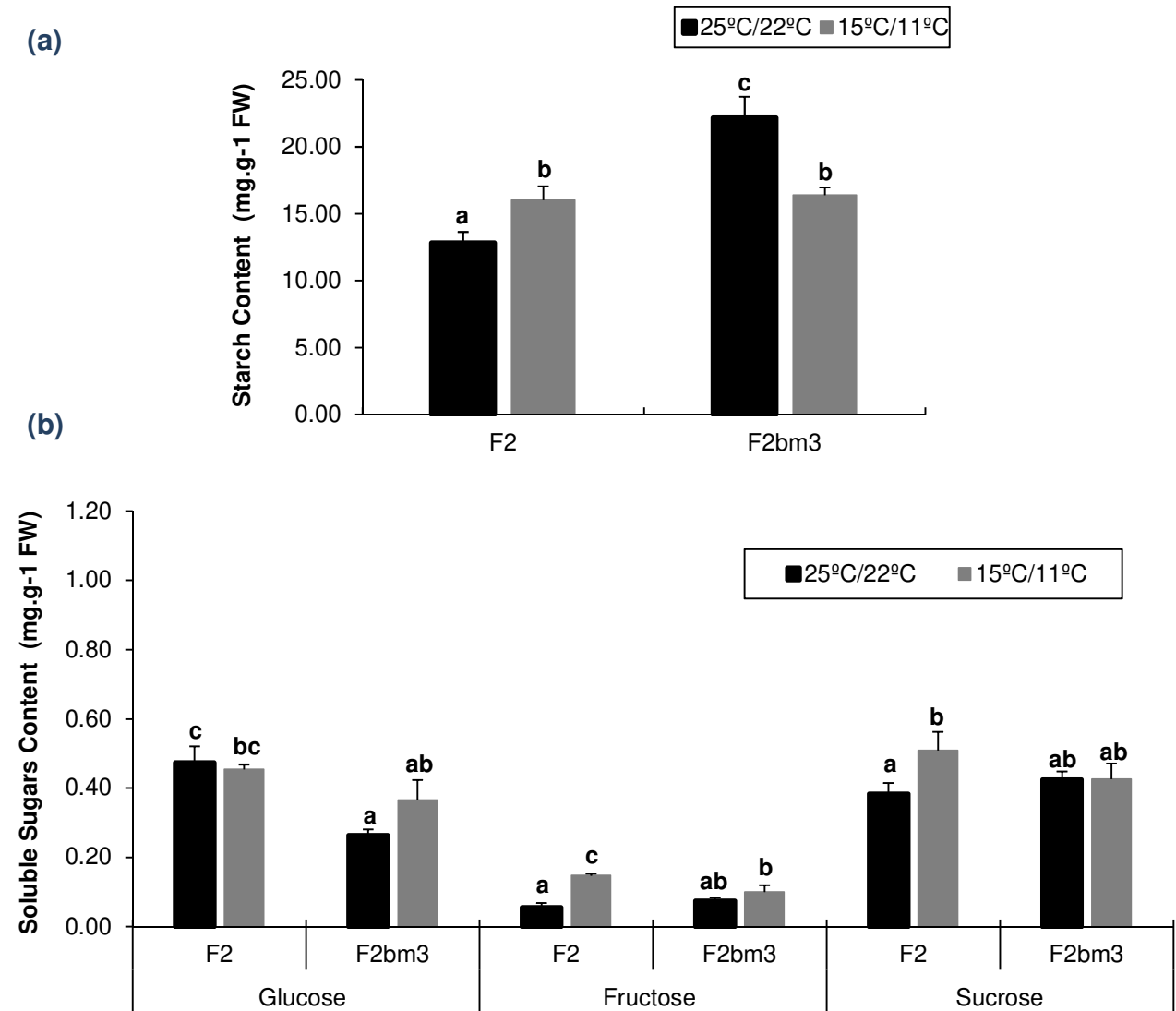


Figure 2. Concentration of non-structural carbohydrates (NSC, (mg. g⁻¹ FW)) under ambient temperature (black bar) and chilling conditions (grey bar). (a) starch and (b) glucose, fructose and sucrose. Data are means \pm SD (n=3). Means followed by the different letters in the same graph are significantly different according to Tukey's test (P<0.05).

3.4. Chilling changes cell wall sugar composition in both F2 and F2*bm3*.

The cellulose content was similar in both F2*bm3* and F2 under control conditions. While the cellulose content did not change in F2*bm3*, a reduction of 25% was observed in F2 as a result of a chilling treatment (**Table 2**). The β -glucan was low and estimated to be around $\pm 0.6\%$ of dry cell wall material in both lines. An increase in the level of β -glucan up to 22% was observed in both F2*bm3* and F2 plants in response to chilling (**Table 2**). No significant variations were observed in the non-cellulosic sugar content in either line under control conditions, indicating that the reduced *COMT* activity in maize does not impact the non-cellulosic sugar content at a juvenile stage. However, the content of non-cellulosic sugars changed in response to chilling with a reduction in xylose (24-26 mol%) and an increase of arabinose (43-46 mol%) in both lines (**Table 2**). As GAX is the major cross-linking glycan of the walls of grasses, the mol% of Ara and Xyl was combined to estimate the relative proportions of this polysaccharide and the relative degree of branching from the ratio of Ara/Xyl was carried out according to Christensen et al. (2010). Under control conditions, the GAX content was approximately 81 mol% in both F2 and F2*bm3* and remained steady in plants exposed to chilling (**Table 2**). Under chilling conditions, the degree of substitution of GAX with arabinofuranosyl residues increased 2-fold in both lines. Thus, under chilling temperature, arabinosyl residues would be progressively added, thus increasing the interaction with ester-bound phenolics.

Table 2. Cell wall sugar composition of the 4th leaf of F2 and F2*bm3* seedlings at the V4 stage. Data are means \pm SD (n=3). Means followed by different letters are significantly different according to Tukey's test (P<0.05). L-Rhamnose (Rha), L-arabinose (Ara), D-galactose (Gal), D-glucose (Glc), D-galacturonic acid (GalUA), D-glucuronic acid (GlcUA), D-Xylose (Xyl).

Trait	F2				F2 <i>bm3</i>			
	25°C/22°C		15°C/11°C		25°C/22°C		15°C/11°C	
	Mean \pm SD		Mean \pm SD		Mean \pm SD		Mean \pm SD	
Cellulose (% of DCW)	19.0 \pm 1.3	b	14.2 \pm 1.2	a	19.6 \pm 1.8	b	19.8 \pm 2.3	b
β -glucan (% of DCW)	0.6 \pm 0.0	a	0.8 \pm 0.0	c	0.6 \pm 0.0	a	0.7 \pm 0.0	b
Non-cellulosic monosaccharide (% mole)	Mean \pm SD		Mean \pm SD		Mean \pm SD		Mean \pm SD	
Rha	0.7 \pm 0.2	a	0.8 \pm 0.3	a	0.7 \pm 0.1	a	0.8 \pm 0.4	a
Ara	14.7 \pm 3.6	a	27.4 \pm 4.3	b	15.8 \pm 1.1	a	27.7 \pm 3.8	b
Gal	2.8 \pm 1.1	a	4.3 \pm 1.3	a	3.2 \pm 0.5	a	4.1 \pm 1.0	a
Glc	12.0 \pm 3.8	a	14.5 \pm 2.6	a	10.9 \pm 3.2	a	13.7 \pm 2.5	a
GalUA	2.2 \pm 0.5	a	3.1 \pm 1.0	a	2.6 \pm 0.5	a	2.9 \pm 0.9	a
GlcUA	1.3 \pm 0.2	a	1.4 \pm 0.4	a	1.2 \pm 0.2	a	1.4 \pm 0.4	a
Xyl	66.2 \pm 7.6	b	48.6 \pm 7.1	a	65.6 \pm 3.9	b	49.6 \pm 7.2	a
Ara + Xyl	80.9 \pm 4.9	a	76.0 \pm 4.8	a	81.3 \pm 3.7	a	77.3 \pm 4.7	a
Ara / Xyl	0.2 \pm 0.1	a	0.6 \pm 0.2	b	0.2 \pm 0.0	a	0.6 \pm 0.1	b

3.5. Chilling does not change lignin content but modifies its composition in F2*bm3*

The amount of lignin in leaves was slightly reduced (13%) in the F2*bm3* mutant compared to F2, under control conditions (**Table 3**). The F2*bm3* mutant had a lower S:G ratio than the F2 plants, as a result of the reduced COMT activity. In plants exposed to chilling content of lignin did not significantly change and the difference in lignin content was maintained (**Table 3**). However, the content of H-residues in the lignin increased by 14% in F2*bm3* plant exposed to chilling, compared to a strong

reduction (72%) in F2 plants. The amount of G and S units did not significantly change in response to chilling in either of the lines, although there was a small increase in S units in F2, compared to an even further reduction in F2*bm3*.

The enzyme responsible for catalyzing the final step of the monolignol biosynthetic pathway, CAD was assayed. Under control conditions CAD activity was almost twice as high in F2*bm3* than in F2, (**Fig. 3**), but under chilling CAD activity increased by 38% in the F2 line to reach a similar CAD enzyme activity level as observed in F2*bm3*.

Table 3. Lignin content and subunit composition (H, G and S residues (%)) determined by thioacydolysis in the 4th leaf of F2 and F2*bm3* seedlings at the V4 stage. Data are means±SD (n=3). Means followed by different letters are significantly different according to Tukey's test (P<0.05).

Trait	F2				F2 <i>bm3</i>			
	25°C/22°C		15°C/11°C		25°C/22°C		15°C/11°C	
	Mean ± SD		Mean ± SD		Mean ± SD		Mean ± SD	
<i>Lignin (% of DCW)</i>	18.4 ± 1.1	c	17.6 ± 0.7	bc	15.9 ± 0.6	ab	14.7 ± 0.8	a
<i>Lignin subunits (%)</i>	Mean ± SD		Mean ± SD		Mean ± SD		Mean ± SD	
<i>H</i>	7.0 ± 0.1	ab	2.0 ± 0.0	a	0.0 ± 0.0	a	14.0 ± 0.0	b
<i>G</i>	64.0 ± 0.1	a	59.0 ± 0.0	a	82.0 ± 0.1	a	73.0 ± 0.1	a
<i>S</i>	29.0 ± 0.1	ab	39.0 ± 0.0	b	18.0 ± 0.1	a	13.0 ± 0.0	a
<i>S/G</i>	0.5 ± 0.2	ab	0.7 ± 0.1	b	0.2 ± 0.2	a	0.2 ± 0.1	a

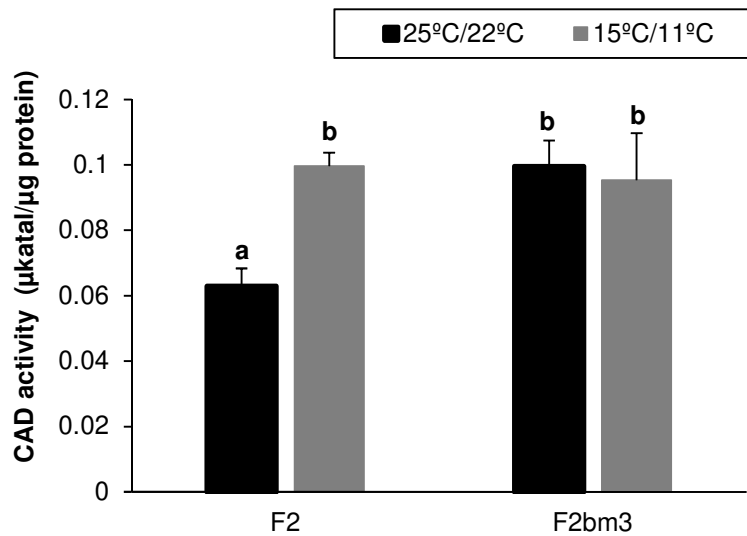


Figure 3. Cinnamyl alcohol dehydrogenase (CAD) enzyme activity assays in the 4th leaf of F2 and F2bm3 seedlings at the V4 stage. Activity is expressed in μkat per μg of protein. Data are means \pm SD ($n=3$). Means followed by different letters are significantly different according to Tukey's test ($P<0.05$). Black columns represent the experiment under ambient temperature and grey columns under exposure to chilling.

3.6. Chilling increases the concentration of cell-wall-bound ferulic acid

Cell wall-bound hydroxycinnamates (HCA) including esterified and etherified FA and pCA were determined by alkaline hydrolysis (Sun et al., 2002; Culhaoglu et al., 2011). The amount of cell-wall-bound HCA was low, reflective of the developmental stage of the plants. No significant changes were observed in either genotype in response to chilling. Under control conditions, on average total FA was more abundant in the F2bm3 mutant (0.4 ± 0.1) than in F2 (0.3 ± 0.1), even though these differences were not

statistically significant (**Table 4**). Following exposure to chilling the average concentration of ester-bound forms increased 3- and 2-fold in F2 and F2*bm3*, respectively, as arabinose content doubled in both lines, while on average the ether-bound forms of FA increased by 1.6-fold in F2*bm3*. FA is ester-linked to arabinose (Ara) units on GAX (Hatfield et al., 2017). In both conditions and in both lines the FA ester/Ara ratio remained unchanged.

Under control conditions the ester-bound and etherified pCA contents in the F2*bm3* samples were half of what was observed for F2 even though these differences were not statistically significant (**Table 4**). Most pCA esters are associated with syringyl residues in the lignin (Ralph et al., 1994). Due to the reduced COMT activity in the F2*bm3* plants, these plants contain less lignin with fewer syringyl residues, and therefore less esterified pCA. (**Table 4**). When the plants were exposed to chilling, esterified and etherified pCA content did not change in the F2*bm3* mutant, while a reduction by 40% was observed in F2 for the ether forms of pCA. These data indicate a reduction of lignin *p*-coumaroylation in F2.

Table 4. Content of cell wall-bound hydroxycinnamates in the 4th leaf of F2 and F2*bm3* seedlings at the V4 stage. Data are means \pm SD (n=3). Means followed by different letters are significantly different according to Tukey's test (P<0.05). Ferulic acid (FA), *p*-coumaric acid (pCA), arabinose (Ara).

<i>Trait (mg.g⁻¹ DW)</i>	F2				F2<i>bm3</i>				
	25°C/22°C		15°C/11°C		25°C/22°C		15°C/11°C		
	Mean	\pm SD	Mean	\pm SD	Mean	\pm SD	Mean	\pm SD	
<i>FA (Ester)</i>	0.1	\pm 0.1	a	0.4	\pm 0.1	ab	0.2	\pm 0.1	ab
<i>FA (Ether)</i>	0.1	\pm 0.1	a	0.1	\pm 0.0	a	0.2	\pm 0.0	a
<i>TOTAL FA</i>	0.3	\pm 0.1	a	0.5	\pm 0.1	ab	0.4	\pm 0.1	ab
<i>pCA (Ester)</i>	0.7	\pm 0.1	a	0.4	\pm 0.0	b	0.3	\pm 0.1	a
<i>pCA (Ether)</i>	0.5	\pm 0.1	b	0.3	\pm 0.2	a	0.3	\pm 0.0	ab
<i>TOTAL pCA</i>	1.1	\pm 0.1	a	0.6	\pm 0.4	a	0.6	\pm 0.1	a
<i>TOTAL FA + pCA</i>	1.4	\pm 0.2	a	1.1	\pm 0.5	a	1.0	\pm 0.2	a

<i>pCA/FA</i>	4.9 ± 2.5	<i>b</i>	1.2 ± 0.6	<i>a</i>	1.6 ± 0.7	<i>ab</i>	0.9 ± 0.3	<i>a</i>
<i>FA ester /Ara</i>	0.0 ± 0.0	<i>a</i>	0.0 ± 0.0	<i>a</i>	0.0 ± 0.0	<i>a</i>	0.0 ± 0.0	<i>a</i>

DISCUSSION

This study characterized changes in photosynthetic and cell wall metabolism in the *F2bm3* mutant exposed to a long chilling treatment during early development. The aim was to better understand how this mutant at an early developmental stage, i.e. when the 4th leaf was fully elongated, could cope with a long chilling stress using as criteria photosynthetic metabolism and cell wall composition. To our knowledge, there is no data on the effects of a long chilling treatment on cell wall and photosynthetic metabolisms in the maize *bm3* mutant. Chilling is an important constraint during early seedling growth. It slows down physiological processes, including photosynthesis, leading to a reduction in biomass production (Guan et al., 2009; Bano et al., 2015; Riva-Roveda et al., 2016; Cholakova-Bimbalova and Vassilev, 2017). In our study, the plant growth was significantly reduced in both genotypes under chilling treatment and the plants did not present any strong chilling injury (**Fig.1, Fig. S1**). The photosynthetic capacity was lower in both lines (**Table S1**). This was characterized by a reduction in PSII efficiency as shown by a decrease in electron transport (Φ PSII). The increase of Φ NPQ in both lines suggests that the dissipation of the excess energy is regulated in both lines under chilling exposure. The decrease in photosynthetic capacity has already been observed in maize under chilling exposure and could be a strategy to reduce photoinhibition (Riva-Roveda et al., 2016, Duran Garzon et al., 2020).

Chilling also causes chlorophyll degradation in maize (Riva-Roveda et al., 2016; Cholakova-Bimbalova and Vassilev, 2017, Duran Garzon et al., 2020). However, in cold-tolerant maize genotypes, chlorophyll and xanthophyll contents are higher (Haldimann, 1998; Fracheboud et al., 1999; Duran-Garzon et al., 2020). The total chlorophyll content remained significantly unchanged in *F2bm3* and F2 in both conditions (**Table 1**). The level of Chl *b* was higher in *F2bm3* than in F2 under control conditions which could increase light harvesting antenna. This could explain the slightly greater plant height in *F2bm3*. A similar trend was observed with chl *a*. Tobacco plants in which the genes encoding CCR and CAD had been downregulated showed an increase in chlorophylls, particularly *chl a* and in Φ PSII, associated with an increase in PSII efficiency (Dauwe et al., 2007). Thus, an alteration of the lignin biosynthesis pathway, as observed in *F2bm3*, may have an interaction with the methylerythritol phosphate pathway (MEP), which is involved in photosynthetic pigments biosynthesis. Furthermore, *F2bm3* contained less xanthophylls than F2 under both growing conditions. The higher level of lutein observed in F2 under chilling could play a significant role in protecting the photosynthetic apparatus from photoinhibition and photooxidation by dissipating excess light energy and eliminating ROS under stress conditions (Song et al., 2016). The level of lutein known to deactivate triplet chlorophyll ($^3\text{Chl}^*$), (Jahns and Holzwarth, 2012) was twice lower in *F2bm3* than in F2 which could reduce the photoprotection of PSII. However, the level of β -carotene observed in *F2bm3* was twice as high as in F2 under chilling and could be another strategy to contribute to photosystem protection (Cazzaniga et al., 2016). Indeed, β -carotene, has the capacity to quench singlet oxygen, scavenge free radicals (Cazzaniga et al., 2012). Thus, the

higher β -carotene content associated with higher *chl a/ chl b* ratio observed in *F2bm3* is a strategy of photoprotection in response to chilling (Haldimann, 1998; Fracheboud et al., 2002). Meanwhile, F2, but not *F2bm3*, showed an increase in neoxanthin. Neoxanthin serves as the main precursor for stress-induced ABA production and could quickly activate cold stress response in F2 through regulation of a set of specific cold-responsive genes (Janowiak et al., 2003). Thus, the photosynthetic machinery is maintained in both lines, but F2 and *F2bm3* adopt a different strategy in photosynthetic pigments biosynthesis with more xanthophyll in F2, and a higher carotene content in *F2bm3* to cope with chilling. The different strategy to protect the photosystem adopted in each genotype is related to the reduction in the proportion of S-residues in the lignin, revealing a pleiotropic effect between photosynthetic pigments and lignin biosynthesis. In the maize *F2bm3* mutant, a reduction of the flavonolignin unit derived from tricetin has been reported, indicating that COMT participates in tricetin biosynthesis (Fornalé et al., 2017). Similar results have been observed in the sorghum *bmr12* mutant, a *comt* mutant (Bout and Vermerris, 2003), in which a lower level of tricetin is incorporated into lignin (Eudes et al., 2017). Tricetin and other flavones have been reported to have a possible role in plant defense (Bing et al., 2007; Li et al., 2020). In winter wheat, the tricetin content decreased during cold acclimation. The authors explained a possible shift in the methylation of tricetin to 5-hydroxyferulic acid by TaOMT2, a flavonoid OMT, which is also implicated in lignin biosynthesis, to reinforce lignin deposition during cold acclimation (Moheb et al., 2013). So, it cannot be excluded that *F2bm3* maize responds differently to chilling because of altered flavone profiles. These flavones could contribute, as many flavonoids, to the protection of the photosynthetic apparatus.

A reduction in temperature can alter carbon partitioning. An accumulation of non-structural sugars is known to occur in maize leaves exposed to chilling (Riva-Roveda et al., 2016, Duran Garzon et al., 2020). Bilska-Kos et al. (2016) showed that transcripts related to plasmodesmata, intercellular transport or phloem loading, and sucrose transporters were downregulated. This was more pronounced in cold-sensitive maize genotypes. We observed that *F2bm3* contained higher amounts of non-structural sugars due to higher starch content under normal growth conditions than F2, indicating that an alteration in the lignin biosynthetic pathway can change carbon metabolism and carbon partitioning (**Table S2**). When the plants were exposed to chilling, the starch content in *F2bm3* leaves decreased and that was associated with an increase of total amylase activity (**Fig.2, Fig. S2**). In *Arabidopsis*, it has been shown that a beta-amylase gene, *AtBMY8/AtBAM3* was induced in response to cold, thus leading to the degradation of starch to maltose, which could contribute to the protection of the electron transport chain and proteins in the chloroplast (Kaplan and Guy, 2005; Thalmann and Santelia, 2017). Thus, the decrease in starch related to a higher amylase activity, and a likely increased level of glucose, observed in *F2bm3* (**Fig.2**), during a long chilling treatment, could contribute to a better photoprotection as more photoprotectants.

It has been also reported that cold or chilling can inhibit photoassimilate translocation in maize (Bilska and Sowiński, 2010; Bilska-Kos et al., 2016). It can thus delay enzyme activities involved in sucrose-starch partitioning. The increased content in soluble sugars (sucrose and fructose) in F2 could contribute to the osmotic homeostasis of the cells in response to a long chilling exposure (Rosa et al., 2009; Yuanyuan et al., 2009). Similarly, the increase in glucose likely observed in *F2bm3* could play a role in osmotic

adjustment in response to chilling. Soluble sugars can also feed NADPH-producing metabolic pathways, such as the oxidative pentose-phosphate (OPP) pathway, which can contribute to ROS scavenging, maintaining homeostasis in response to cold (Scharte et al., 2009). Thus, accumulation of soluble sugars also suggests a reduction in resource remobilization and therefore impairment in growth or biomass accumulation, which could explain the plant growth alteration and reduction in biomass observed in both F2 and F2*bm3*.

Chilling has also an effect on structural cell wall sugars (Le Gall et al., 2015). The content of non-cellulosic sugars was similar in both F2*bm3* and F2 under normal growth conditions (**Table 2**). The cell wall composition in juvenile leaf blades of maize is in agreement with the literature. Indeed, the main non-cellulosic sugars found are xylose, arabinose and glucose (Sindhu et al., 2007). In other studies the level of glucose is higher than in our data (Abedon et al., 2006; Jung and Casler, 2006). Such a discrepancy could be due to the different analytical procedures to quantify non-cellulosic materials. In our case, our values are based only on structural sugar constituents. Cell wall sugar analysis of a maize *bm3* mutant (in the inbred line A619) has been performed before, but at a later developmental stage and on stalks (Marita et al., 2003). However, the main non-cellulosic sugar profile is similar to what was observed in our study. When plants were exposed to chilling, a higher degree of arabinose substitution on the xylan backbone in both genotypes was observed. The degree of branching of GAX could maintain the hydration status of cell wall. However, arabinose can also arise from pectin, although maize has low amount (10%) of pectin or arabinogalactan protein (Santiago et al., 2013). A study on a chilling sensitive maize inbred line, showed that a

short chilling exposure of 3 days caused a reduction in pectin content and PME activity due to change of osmotic potential of the young seedling leaves (Bilska-Kos et al., 2017). In our study, we did not observe any difference in PME enzyme activity between the two genotypes and the two growth temperature conditions (data not shown). That discrepancy could depend on the maize genotype studied and the duration of the chilling treatment, which was much longer in our study. The β -glucan content was increased in both inbred lines in response to chilling. Similar results have been observed in a chilling tolerant maize line and in different *Miscanthus* genotypes after cold exposure (Domon et al., 2013; Bilska-Kos et al., 2018). A reduction of 25% in cellulose content was observed in F2 while the cellulose content remained the same in F2*bm3* after chilling exposure. According to Bilska-Kos et al. (2018), chilling does not affect the cellulose content in the leaves of chilling-tolerant S68911 and chilling-sensitive B73 maize lines at the third fully developed leaf following 3 days of chilling. The discrepancy could be related to the differences in maize genotypes and the duration of the stress. All these data indicate changes in cell wall properties in both genotypes. But some differences in cell wall composition observed between the two lines, including a reduction in cellulose in the F2 line under chilling exposure, reveal different cell wall properties between F2*bm3* and F2 in response to chilling.

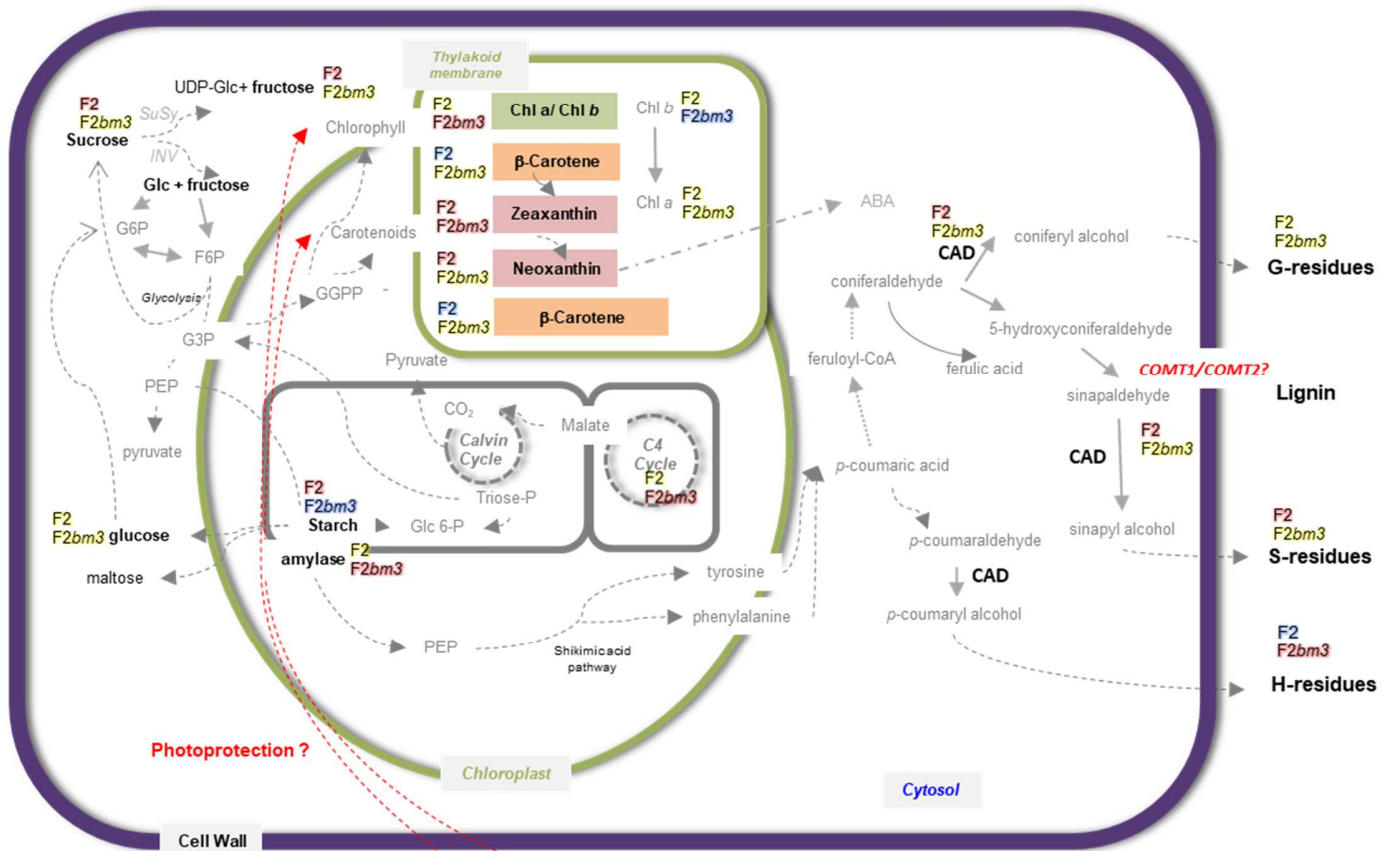
Chilling is often associated with lignin deposition to strengthen the cell wall (Moura-Sobczak et al., 2011; Cabané et al., 2012; Le Gall et al., 2015). Lignin biosynthesis can be enhanced during cold acclimation and participate in cell wall modification by strengthening it, thus preventing freezing damage and cell collapse (Le Gall et al., 2015). Lignin and hydroxycinnamic acids could also scavenge reactive oxygen species

(Grace and Barry, 2000). A proteomic study on pea root showed an accumulation of enzymes involved in lignin biosynthesis, including COMT, in response to a long chilling exposure (8 days) (Badowiec et al., 2013). In our study, we did not observe a significant difference in lignin content as a result of chilling, but only between genotypes, as expected (**Table 3**). Furthermore, our study was performed on leaves at the juvenile stage, where lignin is not abundant. As expected, the leaves of F2 contained more lignin, and with likely a greater proportion of S-units. Following chilling, lignin in F2*bm3* contained higher levels of H-units. The increase in CAD enzyme activity observed in F2 in response to chilling suggests increased monolignol biosynthesis, including sinapyl alcohol, the monolignol giving rise to S-units (**Fig. 3**). Since the lignin content does not change in response to chilling, we could assume a reduced amount of hydroxycinnamaldehydes due to reduced activity in any monolignol biosynthetic enzymes upstream CAD but also downstream as laccase and/or peroxidase thus, limiting the incorporation of these extra monolignols into lignin. In barley leaves, the expression of genes encoding monolignol biosynthetic enzymes, including CAD, was upregulated under cold stress (Janská et al., 2011). These authors suggested that monolignols rather than lignin were synthesized, since peroxidase genes involved in lignin biosynthesis were down-regulated. In several *Miscanthus* genotypes displaying a contrasting response to cold, CAD enzyme activity strongly increased during cold acclimation and that was more pronounced in the cold-tolerant genotype (Domon et al., 2013).

The photoprotection observed in F2*bm3* could also arise from an increase in cell wall-bound FA (**Table 4**). In winter wheat leaves exposed to snow, HCA and HCA amides

with antifungal properties are produced, thus protecting the plant against pathogen under snow conditions (Jin et al., 2003). In maize leaves the accumulation of total phenolic acids, including FA, observed during a water deficit in leaves could function as photoprotectors by limiting light penetration into the mesophyll cells, thus reducing chlorophyll excitation (Hura et al., 2008). In another study, the drought tolerant triticale 'Lamberto' contains more cell wall bound ferulic acid and this is correlated to a better resistance of photosynthetic apparatus to water deficit (Hura et al., 2009). The authors suggest that cell wall bound ferulic acid may act as a light filter limiting mesophyll penetration under drought conditions and can support drought adaption by downregulation of leaf growth. Thus, the increase of cell wall bound HCA in *F2bm3* could reinforce its cell wall and thus could play a key role as photoprotectors leading to a reduction of irradiation area and water loss in response to chilling.

Chilling



F2
F2bm3.comt
mutant
Increase
Decrease
Steady

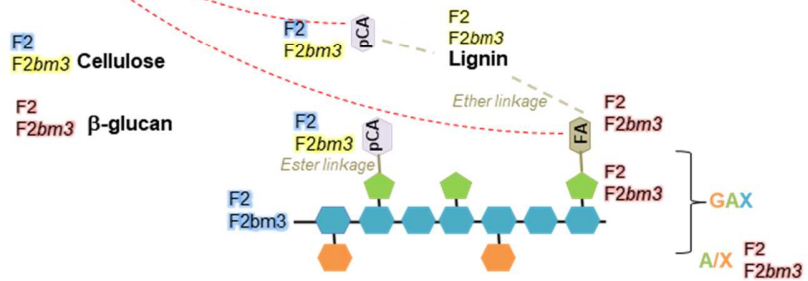


Figure 4: A hypothetical network of interactions within monolignol biosynthesis and photosynthesis, cell wall and carbon metabolisms in the maize low-lignin *brown midrib3* in response to chilling. Changes observed in *F2bm3* and F2 plants are indicated next to each metabolite: In red indicates increased-level/activity, blue decreased level/activity and yellow steady-state level. Partial metabolic pathways are indicated by dashed lines and non-measured metabolites are in grey. A: L-Arabinose; X : D-Xylose ; G : D-Galactose ; GAX: Glucuronoarabinoxylan; FA: Ferulic acid; pCA: *p*-Coumaric acid.

CONCLUSION

In this study, we showed that the reduced COMT activity in the maize mutant *F2bm3* has a pleiotropic effect on photosynthetic and carbohydrate metabolisms (**Figure 4**). *F2bm3* contained more β -carotene under low-temperature conditions. The mutant is capable of starch degradation in response to chilling to provide carbon and energy. The increased levels of cell wall-bound HCA and greater proportion of H-units in the lignin observed in *F2bm3* could reinforce the cell wall, to protect the plant from chilling and the excess of light resulting from chilling as a filter. However, the precise mechanism needs to be elucidated. Despite differences in the levels of photosynthetic pigments, starch and lignin composition between genotypes in response to chilling, vigor did not differ between F2 and *F2bm3* under long moderate chilling, suggesting that CO₂ supply is not a limiting factor in these genotypes. In conclusion, the *F2bm3* mutant is not necessarily more tolerant to chilling than F2, but it uses a different mechanism, suggesting a level of metabolic flexibility to protect against early-season cool temperatures.

Declaration of competing interest

The authors declare no conflict of interest.

Acknowledgements

We are grateful to Dominique Rabier, Jean-François Hu and Benoît Decaux for their help with maize culture, sampling and phenotyping. We thank Solène Bassard for her help in cell wall sugar analysis and Alejandro Lovo for help with the analysis of the thioacidolysis data.

This work was financed by the «Conseil Régional Hauts de France» and « FEDER », in support of the REG15019-COOLBIOM project (2015–2018). We thank Dr Matthieu Reymond (IJPB, INRA Versailles, France) for providing the seeds. The purchase of the GC-MS equipment used for the thioacidolysis was made possible with funding from USDA-NIFA Biomass Research and Development Initiative Grant No. 2011-10006-30358 (WV), the UF Genetics Institute and the UF Department of Molecular Genetics & Microbiology.

Authors' contribution

CR, JMD, and CG designed the experiments. HSR generated plant material. CDG and CG performed photosynthetic activity. CDG, ML, QC, FF and LB carried out cell wall sugar composition, photosynthetic pigment and non-structural sugars analysis. JMD performed lignin content and CAD activity, WV performed thioacidolysis. CDG performed the statistical analysis. CDG, CR, WV and JMD analyzed and interpreted the

data. CDG, CR, JMD and WV wrote the manuscript. All authors read and approved the manuscript.

References

Abedon, B.G., Hatfield, R.D., Tracy, W.F. 2006. Cell wall composition in juvenile and adult leaves of maize (*Zea mays* L.). *J. Agric. Food Chem.* 54, 3896–3900. <https://doi.org/10.1021/jf052872w>.

Badowiec, A., Swigonska, S., Weidner, S., 2013. Changes in the protein patterns in pea (*Pisum sativum* L.) roots under the influence of long- and short-term chilling stress and post-stress recovery. *Plant Physiol. Biochem.* 71, 315–324. <https://doi.org/10.1016/j.plaphy.2013.08.001>.

Bano, S., Aslam, M., Saleem, M., Basra, S.M.A., Aziz, K., 2015. Evaluation of maize accessions under low temperature stress at early growth stages. *J. Anim. Plant Sci.* 25, 392–400.

Barrière, Y., Argillier, O., Chabbert, B., Tollier, M., Monties, B., 1994. Breeding silage maize with brown-midrib genes. Feeding value and biochemical characteristics. *Agronomie* 14, 15–25. <https://hal.archives-ouvertes.fr/hal-00885607>.

Barrière, Y., 2017. Brown-midrib genes in maize and their efficiency in dairy cow feeding. Perspectives for breeding improved silage maize targeting gene modifications in the monolignol and p-hydroxycinnamate pathways. *Maydica* 62, 1–19. <https://hal.archives-ouvertes.fr/hal-01595409>.

Barros, J., Serk, H., Granlund, I., Pesquet, E., 2015. The cell biology of lignification in higher plants. *Ann. Bot.* 115, 1053–1074. <https://doi:10.1093/aob/mcv046>.

Barros, J., Serrani-Yarce, J.C., Chen, F., Baxter, D., Venables, B.J., Dixon, R.A., 2016. Role of bifunctional ammonia-lyase in grass cell wall biosynthesis. *Nat. Plants* 2, 16050. <https://doi:10.1038/nplants.2016.50>.

Bilska, A., Sowiński, P., 2010. Closure of plasmodesmata in maize (*Zea mays*) at low temperature: a new mechanism for inhibition of photosynthesis. *Ann. Bot.* 106, 675–686. <https://doi.org/10.1093/aob/mcq169>.

Bilska-Kos, A., Grzybowski, M., Jończyk, M., Sowiński, P., 2016. In situ localization and changes in the expression level of transcripts related to intercellular transport and phloem loading in leaves of maize (*Zea mays* L.) treated with low temperature. *Acta Physiol. Plant.* 38, 123–133. <http://dx.doi.org/10.1007/s11738-016-2151-5>

Bilska-Kos, A., Solecka, D., Dziejulska, A., Ochodzki, P., Jończyk, M., Bilski, H., Sowiński, P., 2017. Low temperature caused modifications in the arrangement of cell wall pectins due to changes of osmotic potential of cells of maize leaves (*Zea mays* L.). *Protoplasma* 254, 713–724. <https://doi.org/10.1007/s00709-016-0982-y>.

Bilska-Kos, A., Panek, P., Szulc-Głaz, A., Ochodzki, P., Cisło, A., Zebrowski, J., 2018. Chilling-induced physiological, anatomical and biochemical responses in the leaves of *Miscanthus × giganteus* and maize (*Zea mays* L.). *J. Plant Physiol.* 228, 178–188. <https://doi.org/10.1016/j.jplph.2018.05.012>.

Bing, L., Hongxia, D., Maoxin, Z., Di, X., Jingshu, W., 2007. Potential resistance of tricin

in rice against brown planthopper *Nilaparvata lugens* (Stal), *Acta Ecol. Sin.* 27, 1300–1306. [http://dx.doi.org/10.1016/S1872-2032\(07\)60031-6](http://dx.doi.org/10.1016/S1872-2032(07)60031-6).

Boerjan, W., Ralph, J., Baucher, M., 2003. Lignin Biosynthesis. *Annu. Rev. Plant Biol.* 54, 519–546. <https://doi:10.1146/annurev.arplant.54.031902.134938>.

Bout, S., Vermerris, W., 2003. A candidate-gene approach to clone the sorghum *Brown midrib* gene encoding caffeic acid *O*-methyltransferase. *Mol Gen Genomics* 269, 205–214. <https://doi.org/10.1007/s00438-003-0824-4>.

Cabané, M., Afif, D., Hawkins, S., 2012. Lignins and abiotic stresses. *Adv. Bot. Res.* 61, 219–262. <https://doi:10.1016/B978-0-12-416023-1.00007-0>.

Carpita, N.C., Defernez, M., Findlay, K., Wells, B., Shoue, D.A., Catchpole, G., Wilson, R.H., McCann, M.C., 2001. Cell wall architecture of the elongating maize coleoptile. *Plant Physiol.* 127, 551–565. <https://doi:10.1104/pp.010146>.

Carpita, N.C., Gibeaut, D.M., 1993. Structural models of primary cell walls in flowering plants: consistency of molecular structure with the physical properties of the walls during growth. *Plant J.* 3, 1–30. <https://doi:10.1111/j.1365-313X.1993.tb00007.x>.

Cazzaniga, S., Li, Z., Niyogi, K. K., Bassi, R., Dall'Osto, L., 2012. The *Arabidopsis* *szl1* mutant reveals a critical role of β -carotene in photosystem I photoprotection. *Plant Physiol.* 159, 1745–1758. <https://dx.doi.org/10.1104%2Fpp.112.201137>

Cazzaniga, S., Bressan, M., Carbonera, D., Agostini, A., Dall'Osto, L., 2016. Differential roles of carotenes and xanthophylls in photosystem I photoprotection. *Biochemistry* 55, 3636–3649. <https://doi.org/10.1021/acs.biochem.6b00425>.

Chabbert, B., Tollier, M.T., Monties, B., Barrière, Y., Argillier, O., 1994. Biological variability in lignification of maize: Expression of the brown midrib *bm3* mutation in three maize cultivars. *J. Sci. Food Agric.* 164, 349–355. <https://doi.org/10.1002/jsfa.2740640317>.

Cholakova-Bimbalova, R., Vassilev, A., 2017. Effect of chilling stress on the photosynthetic performance of young plants from two maize (*Zea mays*) hybrids. *CBU Int. Conf. Proc.* 5, 1118. <https://doi.org/10.12955/cbup.v5.1081>.

Christensen, U., Alonso-Simon, A., Scheller, H.V., Willats, W.G.T., Harholt, J., 2010. Characterization of the primary cell walls of seedlings of *Brachypodium distachyon* – A potential model plant for temperate grasses. *Phytochem.* 71, 62–69. <https://doi.org/10.1016/j.phytochem.2009.09.019>.

Cui K.H., Peng S.B., Xing Y.Z., Xu C.G., Yu S.B., Zhang Q., 2002. Molecular dissection of seedling-vigor and associated physiological traits in rice. *Theor Appl Genet.* 105, 745–753. <https://doi.org/10.1007/s00122-002-0908-2>.

Culhaoglu, T., Zheng, D., Méchin, V., Baumberger, S., 2011. Adaptation of the Carrez procedure for the purification of ferulic and p-coumaric acids released from lignocellulosic biomass prior to LC/MS analysis. *J. Chromatogr. B Analyt. Technol. Biomed. Life Sci.* 879, 3017–3022. <https://doi.org/10.1016/j.jchromb.2011.08.039>.

Dauwe, R., Morreel, K., Goeminne, G., Gielen, B., Rohde A., Van Beeumen, J., Ralph, J., Boudet, A-M., Kopka, J., Rochange, S., Halpin, C., Messens, E., Boerjan, W., 2007. Molecular phenotyping of lignin-modified tobacco reveals associated changes in cell-wall metabolism, primary metabolism, stress metabolism and photorespiration. *Plant J.* 52, 263–285. [https://doi: 10.1111/j.1365-313X.2007.03233](https://doi:10.1111/j.1365-313X.2007.03233).

de O. Buanafina, M.M., 2009. Feruloylation in grasses: current and future perspectives. *Mol. Plant* 2, 861–872. [https://doi: 10.1093/mp/ssp067](https://doi:10.1093/mp/ssp067).

de Oliveira, D.M., Finger-Teixeira, A., Rodrigues-Mota, T., Salvador, V.H., Moreira-Vilar, F.C., Correa-Molinari, H.B., Craig-Mitchell, R.A., Marchiosi, R., Ferrarese-Filho, O., Dantas dos Santos, W., 2015. Ferulic acid: a key component in grass lignocellulose recalcitrance to hydrolysis. *Plant Biotechnol. J.* 13, 1224–1232. [https://doi: 10.1111/pbi.12292](https://doi:10.1111/pbi.12292).

de Souza, A.P., Arundale, R.A., Dohleman, F.G., Long, S.P., Buckeridge, M.S., 2013. Will the exceptional productivity of *Miscanthus x giganteus* increase further under rising atmospheric CO₂ ? *Agr. Forest Meteorol.* 171–172, 82–92. [https://doi: 10.1016/j.agrformet.2012.11.00](https://doi:10.1016/j.agrformet.2012.11.00).

Domon, J.M., Baldwin, L., Acket, S., Caudeville, E., Arnoult, S., Zub, H., Gillet, F., Lejeune-Hénaut, I., Brancourt-Hulmel, M., Pelloux, J., Rayon, C., 2013. Cell wall compositional modifications of *Miscanthus* ecotypes in response to cold acclimation. *Phytochem.* 85, 51–61. <https://doi.org/10.1016/j.phytochem.2012.09.001>.

Duran-Garzon, C.D., Lequart, M., Rautengarten, C., Bassard, S., Sellier-Richard, H., Baldet, P., Heazlewood, J.L., Gibon, Y., Domon, J.M., Giauffret, C., Rayon, C., 2020.

Regulation of carbon metabolism in two maize sister lines contrasted for chilling tolerance. *J. Exp. Bot.* 71, 356–369. [https://doi: 10.1093/jxb/erz421](https://doi.org/10.1093/jxb/erz421).

Edelenbos, M., Christensen, L.P., Grevsen, K., 2001. HPLC Determination of chlorophyll and carotenoid pigments in processed green Pea cultivars (*Pisum sativum* L.). *J. Agric. Food Chem.* 49, 4768–4774. [https://doi: 10.1021/jf010569z](https://doi.org/10.1021/jf010569z).

Eudes, A., Dutta, T., Deng, K., Jacquet, N., Sinha, A., Benites, V.T., et al., 2017. SbCOMT (Bmr12) is involved in the biosynthesis of tricetin-lignin in sorghum. *PLoS ONE* 12, 6. <https://doi.org/10.1371/journal.pone.0178160>.

Fleischer, A., O'Neill, M.A., Ehwald, R., 1999. The pore size of non-graminaceous plant cell walls is rapidly decreased by borate ester cross-linking of the pectic polysaccharide rhamnogalacturonan II. *Plant Physiol.* 121, 829–838. <https://doi.org/10.1104/pp.121.3.829>.

Fontaine, A.S., Bout, S., Barrière, Y., Vermerris, W., 2003. Variation in cell wall composition among forage maize (*Zea mays* L.) inbred lines and its impact on digestibility. II. Analysis of neutral detergent fiber composition by pyrolysis-gas chromatography-mass spectrometry. *J. Agric. Food Chem.* 51, 8080–8087. <http://dx.doi.org/10.1021/jf034321g>.

Fornalé, S., Rencoret, J., García-Calvo, L., Encina, A., Rigau, J., Gutiérrez, A., Carlos del Río, J., Caparros-Ruiz, D., 2017. Changes in cell wall polymers and degradability in Maize mutants lacking 3'- and 5'-O-methyltransferases involved in lignin biosynthesis. *Plant Cell Physiol.* 58, 240–255. <https://doi.org/10.1093/pcp/pcw198>.

Foster, C.E., Martin, T.M., Pauly, M., 2010a. Comprehensive compositional analysis of plant cell walls (lignocellulosic biomass) Part I: Lignin. *J. Vis. Exp.* 37, 1745. <https://doi:10.3791/1745>.

Foster, C.E., Martin, T.M., Pauly, M., 2010b. Comprehensive compositional analysis of plant cell walls (lignocellulosic biomass) Part II: Carbohydrates. *J. Vis. Exp.* 37, 1837. <https://doi:10.3791/1837>.

Fracheboud, Y., Haldimann, P., Leipner, J., Stamp, P., 1999. Chlorophyll fluorescence as a selection tool for cold tolerance of photosynthesis in maize (*Zea mays* L.). *J. Exp. Bot.* 50, Pages 1533–1540. <https://doi:10.1093/jxb/50.338.1533>.

Fracheboud, Y., Ribaut, J.-M., Vargas, M., Messmer, R., Stamp, P., 2002. Identification of quantitative trait loci for cold-tolerance of photosynthesis in maize (*Zea mays* L.). *J. Exp. Bot.* 53, 1967–1977. <https://doi.org/10.1093/jxb/erf040>.

Fu, C., Mielenz, J.R., Xiao, X., Ge, Y., Hamilton, C.Y., Rodriguez, M., Chen, F., Foston, M., Ragauskas, A., Bouton, J., Dixon, R.A., Wang, Z.Y., 2011. Genetic manipulation of lignin reduces recalcitrance and improves ethanol production from switchgrass. *Proc. Natl. Acad. Sci. USA* 108, 3803–3808. <https://doi.org/10.1073/pnas.1100310108>.

Grace, S.C., Barry A.L., 2000. Energy dissipation and radical scavenging by the plant phenylpropanoid pathway. *Phil. Trans. R. Soc. Lond.* 355, 1499–1510. <https://doi.org/10.1098/rstb.2000.0710>.

Guan, Y., Hu, J., Wang, X., Shao, C., 2009. Seed priming with chitosan improves maize germination and seedling growth in relation to physiological changes under low

temperature stress. *J. Zhejiang Univ. Sci. B.* 10, 427–433. <https://doi.org/10.1631/jzus.B0820373>.

Guillaumie, S., Goffner, D., Barbier, O., Martinant, J.P., Pichon, M., Barrière, Y., 2008. Expression of cell wall related genes in basal and ear internodes of silking brown-midrib-3, caffeic acid O-methyltransferase (COMT) down-regulated, and normal maize plants. *BMC Plant Biol.* 8, 71. <https://doi.org/10.1186/1471-2229-11-163>.

Haldimann, P., 1998. Low growth temperature-induced changes to pigment composition and photosynthesis in *Zea mays* genotypes differing in chilling sensitivity. *Plant Cell Environ.* 21, 200–208. <https://doi.org/10.1046/j.1365-3040.1998.00260.x>.

Hatfield, R.D., Rancour, D.M., Marita, J.M., 2017. Grass cell walls: A story of cross-linking. *Front. Plant Sci.* 7, 2056. <https://doi.org/10.3389/fpls.2016.02056>.

Hatfield, R.D., Wilson, J.R., Mertens, D.R., 1999. Composition of cell walls isolated from cell types of grain sorghum stems. *J. Sci. Food Agric.* 79, 891–899. [https://doi.org/10.1002/\(SICI\)1097-0010\(19990501\)79:6](https://doi.org/10.1002/(SICI)1097-0010(19990501)79:6).

Hura, T., Hura, K., Grzesiak, S., 2008. Contents of total phenolics and ferulic acid, and PAL activity during water potential changes in leaves of maize single-cross hybrids of different drought tolerance. *J. Agron. Crop Sci.* 194, 104–112. <https://doi.org/10.1111/j.1439-037X.2008.00297>.

Hura, T., Hura, K., Grzesiak, S., 2009. Possible contribution of cell-wall-bound ferulic acid in drought resistance and recovery in triticale seedlings. *J. Plant Physiol.* 166, 1720–1733. <https://doi.org/10.1016/j.jplph.2009.04.012>.

Jahns, P., Holzwarth, A.R., 2012. The role of the xanthophyll cycle and of lutein in photoprotection of photosystem II. *Biochim. Biophys. Acta* 1817, 182–193. <https://doi.org/10.1016/j.bbabi.2011.04.012>.

Janowiak, F., Luck, E., Dörffling, K., 2003. Chilling tolerance of maize seedlings in the field during cold periods in spring is related to chilling-induced increase in abscisic acid level. *J. Agr. Crop Sci.* 189, 156–161. <https://doi.org/10.1046/j.1439-037X.2003.00027>.

Janská, A., Aprile, A., Zámečník, J., Cattivelli, L., Ovesná, J., 2011. Transcriptional responses of winter barley to cold indicate nucleosome remodeling as a specific feature of crown tissues. *Funct. Integr. Genomics* 11, 307–325. <https://doi.org/10.1007/s10142-011-0213-8>.

Jin, S., Yoshida, M., Nakajima, T., Murai, A., 2003. Accumulation of Hydroxycinnamic acid amides in winter wheat under snow. *Biosci. Biotechnol. Biochem.* 67, 1245–1249. <https://doi.org/10.1271/bbb.67.1245>.

Jun, S. Y., Sattler, S. A., Cortez, G. S., Vermerris, W., Sattler, S. E., Kang, C., 2018. Biochemical and structural analysis of substrate specificity of a phenylalanine ammonia-lyase. *Plant physiology* 176, 1452-1468. <https://doi.org/10.1104/pp.17.01608>.

Jung, H.G., Casler, M.D., 2006. Maize stem tissues: impact of development on cell wall degradability. *Crop Sci.* 46, 1801–1809. <https://doi.org/10.2135/cropsci2006.02-0086>.

Jung, J.H., Fouad, W.M., Vermerris, W., Gallo, M., Altpeter, F., 2012. RNAi suppression of lignin biosynthesis in sugarcane reduces recalcitrance for biofuel production from

lignocellulosic biomass: RNAi suppression of COMT in sugarcane. *Plant Biotechnol. J.* 10, 1067–1076. <https://doi.org/10.1111/j.1467-7652.2012.00734.x>.

Kaplan, F., Guy, C.L., 2005. RNA interference of *Arabidopsis* beta-amylase prevents maltose accumulation upon cold shock and increases sensitivity of PSII photochemical efficiency to freezing stress: BMY8 and freezing stress. *Plant J.* 44, 730–743. <https://doi.org/10.1111/j.1365-313X.2005.02565>.

Le Gall, H., Philippe, F., Domon, J.M., Gillet, F., Pelloux, J., Rayon, C., 2015. Cell wall metabolism in response to abiotic stress. *Plants* 4, 112–166. <https://doi:10.3390/plants4010112>.

Lapierre, C., Rolando, C., 1988. Thioacidolyses of pre-methylated lignin samples from pine compression and poplar woods. *Holzforschung* 42, 1–4. <https://doi:10.1515/hfsg.1988.42.1.1>.

Leipner, J., Stamp, P., 2008. Chilling stress in maize seedlings, in: Bennetzen, L.J., Hake, S.C. (Eds), *Handbook of Maize: Its Biology*. Springer, New York, pp.291-310. https://doi.org/10.1007/978-0-387-79418-1_15.

Li, H.; Li, D.; Yang, Z.; Zeng, Q.; Luo, Y.; He, N., 2020. Flavones produced by mulberry flavone synthase type I constitute a defense line against the ultraviolet-B stress. *Plants* 9, 215. <https://doi.org/10.3390/plants9020215>.

Marita, J.M., Vermerris, W., Ralph, J., Hatfield, R.D., 2003. Variations in the cell wall composition of maize brown midrib mutants. *J. Agric. Food Chem.* 51, 1313–1321. <https://doi:10.1021/jf0260592>.

McCann, M.C., Carpita, N.C., 2015. Biomass recalcitrance: a multi-scale, multi-factor, and conversion-specific property. *J. Exp. Bot.* 66, 4109–4118. [https://doi: 10.1093/jxb/erv267](https://doi.org/10.1093/jxb/erv267).

Méchin, V., Argillier, O., Menanteau, V., Barrière, Y., Mila, I., Pollet, B., Lapierre, C., 2000. Relationship of cell wall composition to *in vitro* cell wall digestibility of maize inbred line stems. *Sci. Food Agri.* 80, 574–580. [https://doi.org/10.1002/\(SICI\)1097-0010\(200004\)80:5<574::AID-JSFA575>3.0.CO;2-R](https://doi.org/10.1002/(SICI)1097-0010(200004)80:5<574::AID-JSFA575>3.0.CO;2-R).

Méchin, V., Argillier, O., Rocher, F., Hébert, Y., Mila, I., Pollet, B., Barrière, Y., Lapierre, C., 2005. In search of a maize ideotype for cell wall enzymatic degradability using histological and biochemical lignin characterization. *J. Agric. Food Chem.* 53, 5872–5881. <https://doi.org/10.1021/jf050722f>.

Moheb, A., Agharbaoui, Z., Kanapathy, F., Ibrahim, R.K., Roy, R., Sarhan, F., 2013. Tricin biosynthesis during growth of wheat under different abiotic stresses. *Plant Sci.* 201-202, 115-20. <https://doi.org/10.1016/j.plantsci.2012.12.005>.

Moura-Sobczak, J., Souza, U., Mazzafera, P., 2011. Drought stress and changes in the lignin content and composition in *Eucalyptus*. *BMC Proc.* 5, 103. <https://doi.org/10.1186/1753-6561-5-S7-P103>.

Peña, M.J., Kulkarni, A.R., Backe, J., Boyd, M., O'Neill, M.A., York, W.S., 2016. Structural diversity of xylans in the cell walls of monocots. *Planta* 244, 589–606. [https://doi: 10.1007/s00425-016-2527-1](https://doi.org/10.1007/s00425-016-2527-1).

Piquemal, J., Chamayou, S., Nadaud, I., Beckert, M., Barrière, Y., Mila, I., Lapierre, C., Rigau, J., Puigdomenech, P., Jauneau, A., Dignonnet, C., Boudet, A.M., Goffner, D., Pichon, M., 2002. Down-regulation of caffeic acid O-methyltransferase in maize revisited using a transgenic approach. *Plant Physiol.* 130, 1675–1685. [https://doi: 10.1104/pp.012237](https://doi.org/10.1104/pp.012237).

Ralph, J., Hatfield, R.D., Quideau, S., Helm, R.F., Grabber, J.H., Jung, H-J.G., 1994. Pathway of p-coumaric acid incorporation into maize lignin as revealed by NMR. *J. Am. Chem. Soc.* 116, 9448–9456. <https://doi.org/10.1021/ja00100a006>.

Ralph, J., Grabber, J.H., Hatfield, R.D., 1995. Lignin-ferulate cross-links in grasses: active incorporation of ferulate polysaccharide esters into ryegrass lignins. *Carbohydr. Res.* 275, 167–178. [https://doi.org/10.1016/0008-6215\(95\)00237-N](https://doi.org/10.1016/0008-6215(95)00237-N).

Ralph, J., Lundquist, K., Brunow, G., Lu, F., Kim, H., Schatz, P.F., Marita, J.M., Hatfield, R.D., Ralph, S.A., Christensen, J.H., Boerjan, W., 2004. Lignins: Natural polymers from oxidative coupling of 4-hydroxyphenyl- propanoids. *Phytochem. Rev.* 3, 29–60. [https://doi: 10.1023/B:PHYT.0000047809.65444.a4](https://doi.org/10.1023/B:PHYT.0000047809.65444.a4).

Ranum, P., Peña-Rosas, J.P., Garcia-Casa, I. M.N., 2014. Global maize production, utilization, and consumption: Maize production, utilization, and consumption. *Ann N Y Acad Sci* 1312, 105–112. [https://doi: 10.1111/nyas.12396](https://doi.org/10.1111/nyas.12396).

Riva-Roveda, L., Escale, B., Giauffret, C., Périlleux, C., 2016. Maize plants can enter a standby mode to cope with chilling stress. *BMC Plant Biol.* 16, 212. [https://doi: 10.1186/s12870-016-0909-y](https://doi.org/10.1186/s12870-016-0909-y).

Rosa, M., Prado, C., Podazza, G., Interdonato, R., González, J.A., Hilal, M., Prado, F.E., 2009. Soluble sugars: Metabolism, sensing and abiotic stress: A complex network in the life of plants. *Plant Signal Behav.* 4, 388–393. <https://doi.org/10.4161/psb.4.5.8294>.

Rösler, J., Krekel, F., Amrhein, N., Schmid, J., 1997. Maize phenylalanine ammonia-lyase has tyrosine ammonia-lyase activity. *Plant Physiol.* 113, 175–179. [https://doi: 10.1104/pp.113.1.175](https://doi.org/10.1104/pp.113.1.175).

Santiago, R., Barros-Rios, J., Malvar, R., 2013. Impact of cell wall composition on maize resistance to pests and diseases. *Int. J. Mol. Sci.* 14, 6960–6980. <https://doi.org/10.3390/ijms14046960>.

Scharte, J., Schon, H., Tjaden, Z., Weis, E., von Schaewen, A., 2009. Isoenzyme replacement of glucose-6-phosphate dehydrogenase in the cytosol improves stress tolerance in plants. *Proc. Natl. Acad. Sci.* 106, 8061–8066. <https://doi.org/10.1073/pnas.0812902106>.

Scheller, H.V., Ulvskov, P., 2010. Hemicelluloses. *Annu. Rev. Plant Biol.* 61, 263–289. [https://doi:10.1146/annurev-arplant-042809-112315](https://doi.org/10.1146/annurev-arplant-042809-112315).

Sindhu, A., Langewisch, T., Olek, A., Multani, D.S., McCann, M.C., Vermerris, W., Carpita, N.C., Johal, G., 2007. Maize brittle stalk2 encodes a COBRA-Like protein expressed in early organ development but required for tissue flexibility at maturity. *Plant Physiol.* 145, 1444–1459. [https:// doi: 10.1104/pp.107.102582](https://doi.org/10.1104/pp.107.102582).

Song, X., Diao, J., Ji, J., Wang, G., Li, Z., Wu, J., Josine, T.L., Wang, Y., 2016. Overexpression of lycopene epsilon-cyclase gene from lycium chinense confers tolerance to chilling stress in *Arabidopsis thaliana*. *Gene* 576, 395–403. [https://doi: 10.1016/j.gene.2015.10.051](https://doi.org/10.1016/j.gene.2015.10.051).

Sun, R., Sun, X.F., Wang, S.Q., Zhu, W., Wang, X.Y., 2002. Ester and ether linkages between hydroxycinnamic acids and lignins from wheat, rice, rye, and barley straws, maize stems, and fast-growing poplar wood. *Ind. Crops Prod*; 15, 179–188. [https://doi: 10.1016/s0926-6690\(01\)00112-1](https://doi.org/10.1016/s0926-6690(01)00112-1).

Thalman, M., Santelia, D., 2017. Starch as a determinant of plant fitness under abiotic stress. *New Phytol.* 214, 943–951. <https://doi.org/10.1111/nph.14491>.

Torney, F., Moeller; L., Scarpa, A., Wang, K., 2007. Genetic engineering approaches to improve bioethanol production from maize. *Curr. Opin. Biotechno.* 18, 193–199. [https://doi: 10.1016/j.copbio.2007.03.006](https://doi.org/10.1016/j.copbio.2007.03.006).

Torres, A.F., Visser, R.G.F., Trindade, L.M., 2015. Bioethanol from maize cell walls: genes, molecular tools, and breeding prospects. *GCB Bioenergy* 7, 591–607. <https://doi.org/10.1111/gcbb.12164>.

Vanholme, R., Demedts, B., Morreel, K., Ralph, J., Boerjan, W., 2010. Lignin biosynthesis and structure. *Plant Physiol* 153, 895–905. [https://doi:10.1104/pp.110.155119](https://doi.org/10.1104/pp.110.155119).

Vignols, F., Rigau, J., Torres, M.A., Capellades, M., Puigdomènech, P., 1995. The brown midrib3 (bm3) mutation in maize occurs in the gene encoding caffeic acid O-methyltransferase. *Plant Cell* 7, 407–416. <https://doi.org/10.1105/tpc.7.4.407>.

Vermerris, W., Abri, I. A., 2015. Enhancing cellulose utilization for fuels and chemicals by genetic modification of plant cell wall architecture. *Curr. Opin. Biotechnol.* 32, 104–112. <http://doi.org/10.1016/j.copbio.2014.11.024>.

Vermerris, W., Saballos, A., Ejeta, G., Mosier N.S., Ladisch, M.R., Carpita, N., 2007. Molecular Breeding to Enhance Ethanol Production from Corn and Sorghum Stover. *Crop Science* 47, 142–153. <https://doi.org/10.2135/cropsci2007.04.0013IPBS>.

Yuanyuan, M., Yali, Z., Jiang, L., Hongbo, S., 2009. Roles of plant soluble sugars and their responses to plant cold stress. *Afr. J. Biotechnol.* 8, 2004-2010.

Zeng, M., Ximenes, E., Ladisch, M.R., Mosier, N.S., Vermerris, W., Huang, C.P., Sherman, D.M., 2012. Tissue-specific biomass recalcitrance in corn stover pretreated with liquid hot-water: Enzymatic hydrolysis (part 1). *Biotechnol. Bioeng.* 109, 390–397. <http://dx.doi.org/10.1002/bit.23337>.